

# Increased spatial homogeneity in a light-emitting InGaN thin film using optical near-field desorption

T. Yatsui · S. Yamazaki · K. Ito · H. Kawamura ·  
M. Mizumura · T. Kawazoe · M. Ohtsu

Received: 4 September 2009 / Published online: 14 October 2009  
© Springer-Verlag 2009

**Abstract** We report a self-assembly method that produces greater spatial uniformity in InGaN thin films using optical near-field desorption. Spatial homogeneity in the In fraction was reduced by introducing additional light during the photo-enhanced chemical vapor deposition of InGaN. Near-field desorption of InGaN nanoparticles, upon addition depended on the In content of the film, and the photon energy of the illumination source determined the energy of the emitted photons. Since this deposition method is based on a photo-desorption reaction, it can easily be applied to other deposition techniques and used with other semiconductor systems.

**PACS** 68.43.Tj · 81.16.Dn

## 1 Introduction

The control of light-emitting-diode (LED) color is important in many applications, including the generation of

white light [1] and optical communications [2]. The photon energy,  $h\nu_{\text{em}}$ , emitted from a composite semiconductor can be tailored by adjusting its composition. White light-emitting diodes (WLEDs) were developed using gallium nitride (GaN)-based LEDs because the  $h\nu_{\text{em}}$  from GaN can be shifted from 400 nm to 1.5 μm by adjusting the indium (In) content in  $\text{In}_x\text{Ga}_{1-x}\text{N}$  from  $x = 0$  to 1, respectively [1, 3]. Although some commercial WLEDs combine the emission of three colored LEDs, the resulting color-rendering index over a broad spectrum is low due to the low spatial uniformity of In. As a result, this type of WLED has yet to replace fluorescent lamps in many applications. Here we report a self-assembly method that yields greater spatial uniformity of In in InGaN thin films using optical near-field desorption. The spatial heterogeneity of the In fraction was reduced by introducing an additional light source (i.e., a desorption light source) during the photo-enhanced chemical vapor deposition (PECVD) of InGaN, thereby causing near-field desorption of InGaN nanoparticles. The degree of nanoparticle desorption depended on In content of the film, and the photon energy of the desorption light source ultimately determined the emitted photon energy of the thin film.

## 2 Controlling the thin film composition using the optical near field

Figures 1a and b illustrate the approach to obtaining a more spatially uniform device composition using optical near-field effects. During the initial stages of  $\text{In}_{x1}\text{Ga}_{1-x1}\text{N}$  nanoparticle growth (bandgap energy  $E_{x1}$ ), a lattice vibrational mode can be excited by far-field light originating from an optical near field caused by coupling of exciton-polaritons and phonons (Fig. 1a) [4]. If the nanoparticles are

T. Yatsui (✉) · S. Yamazaki · T. Kawazoe · M. Ohtsu  
School of Engineering, The University of Tokyo, Bunkyo-ku,  
Tokyo 113-8656, Japan  
e-mail: [yatsui@ee.t.u-tokyo.ac.jp](mailto:yatsui@ee.t.u-tokyo.ac.jp)

T. Yatsui · T. Kawazoe · M. Ohtsu  
Nanophotonic Research Center, Graduate School of Engineering,  
The University of Tokyo, Bunkyo-ku, Tokyo 113-8656, Japan

K. Ito · H. Kawamura  
Central Research and Development Centre, Nitto Optical Co.,  
Ltd., Senboku-gun, Akita 019-140, Japan

M. Mizumura  
Research and Development Department, V-Technology Co., Ltd.,  
Yokohama, Kanagawa 240-0005, Japan

concurrently illuminated by a desorption source with photon energy of  $h\nu_{x2} (< E_{x1})$ , a strong optical absorption due to a multistep excitation of lattice vibrational modes induces

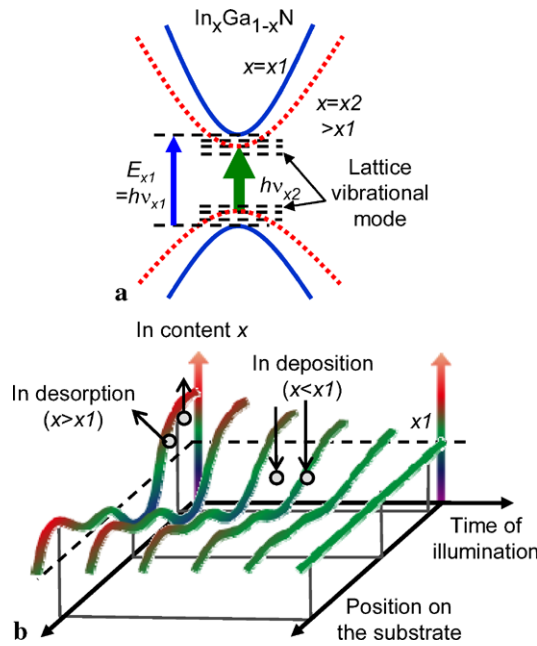


**Fig. 1** Controlling the thin film composition using the optical near field. **a** A schematic diagram shows the energy dispersion and the generation of lattice vibrational modes induced by an optical near field on InGaN nanoparticles. **b** Spatial distributions of  $x$  are shown as a function of deposition time for  $\text{In}_x\text{Ga}_{1-x}\text{N}$  whilst illuminated with the desorption light source

desorption of a fraction of the nanoparticle population [5]. The absorption is enhanced by increasing the In content. As the deposition proceeds with desorption source illumination, the growth is governed by a trade-off between In deposition (where the In content  $x < x_1$ ) and In desorption (where  $x > x_1$ ). Thus, the resulting In content in the film is a function of  $h\nu_{x2}$ , and both spatial heterogeneity of the In fraction and spectral broadening (Fig. 1b) are avoided.

### 3 Experiment

A spectral change was observed upon introduction of the desorption light source during PECVD of InGaN at room temperature [6] in which  $h\nu_{\text{em}}$  was determined by the photon energy  $h\nu_{x2}$ . A 5th-harmonic, Q-switched Nd:YAG laser ( $h\nu_{\text{depo}} = 5.82 \text{ eV}, \lambda = 213 \text{ nm}$ ) was used to excite and photodissociate trimethylgallium (TMG), triethylindium (TEI) and ammonia ( $\text{NH}_3$ , 99.999%). The choice of laser was based on the strong photo-absorptions of gas-phase TMG ( $E_g > 4.59 \text{ eV}$ ), TEI ( $E_g > 4.77 \text{ eV}$ ) and  $\text{NH}_3$  ( $E_g > 5.66 \text{ eV}$ ), respectively [7, 8]. The desorption light source was introduced through an optical window, and  $\text{H}_2$  gas was introduced around the window to prevent GaN deposition onto the window. The substrate was placed at the center of the reaction chamber and irradiated with a 2-mm spot size of excitation light. The total pressure in the reaction chamber was 5.4 Torr, and the deposition time was 60 min.

**Fig. 2** SEM images of fabricated InGaN thin films. The overall image is shown in (a). Magnified images show films fabricated with  $r_{\text{TEI}} = 0$  (b),  $2.5 \times 10^{-3}$  (c),  $5.0 \times 10^{-3}$  (d) sccm

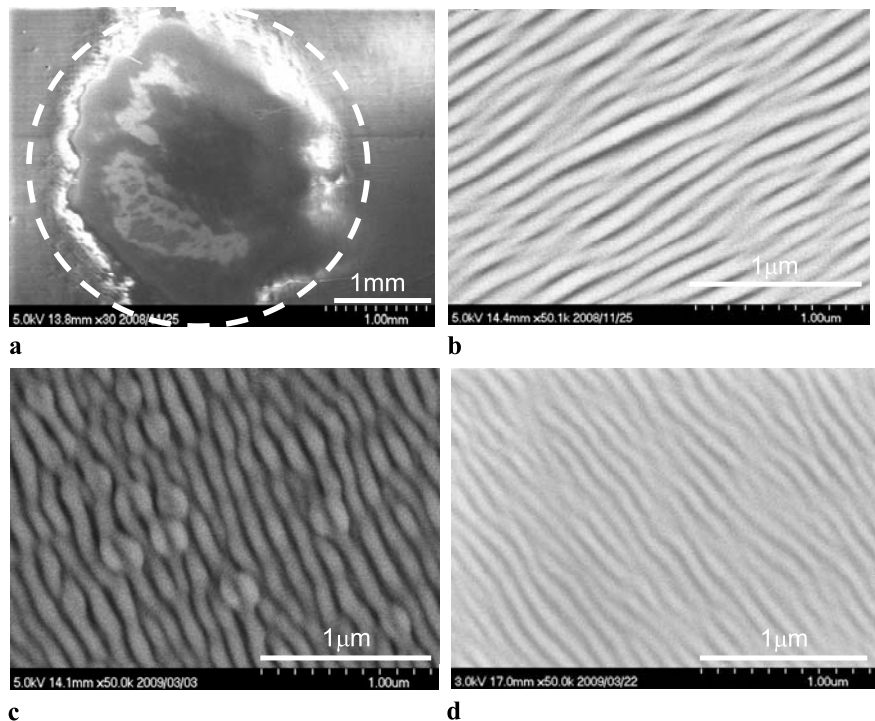
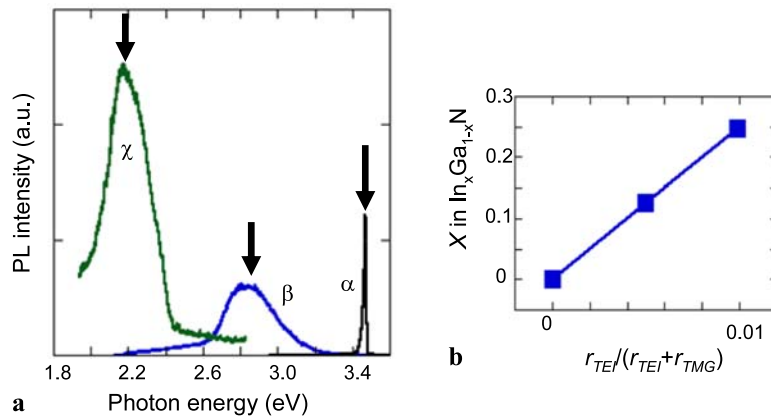


**Fig. 3** Spectral control by adjusting the TEI flow rate,  $r_{TEI}$ , at room temperature. **a** PL spectra obtained at 5 K were acquired following room-temperature film deposition with  $r_{TEI} = 0$  ( $\alpha$ ),  $2.5 \times 10^{-3}$  ( $\beta$ ),  $5.0 \times 10^{-3}$  ( $\chi$ ) sccm with  $r_{TMG} = 0.5$  sccm. **b** The indium content of InGaN shown as a function,  $r_{TEI}$



#### 4 Results and discussion

The morphology of the GaN sample was investigated with a scanning electron microscope (SEM). Figure 2a shows the overall SEM image of the InGaN film on the substrate. Figures 2b through d show magnified SEM images from within the white dashed circle in Fig. 2a. Similar morphologies, consisting of 100-nm lines, were observed at different TEI flow rates,  $r_{TEI}$ . The relative atomic compositions of indium, gallium and nitrogen were obtained by monitoring photoluminescence (PL) induced by a continuous wave He–Cd laser (3.81 eV,  $\lambda = 325$  nm), in which the PL peak was shifted by changing  $r_{TEI}$  (Fig. 3a). The In content,  $x$ , was determined according to

$$E = 3.42 - 4.95x, \quad (1)$$

where  $E$  refers to the PL peak energy [9]. Figure 3b shows that  $x$  was a linear function of  $r_{TEI}$ , which agrees with results obtained using low-temperature metal-organic chemical vapor deposition (MOCVD) [10].

Based on the above results, a spectral shift was induced by introducing desorption light during PECVD. InGaN was grown with  $r_{TEI} = 2.5 \times 10^{-3}$  sccm and under illumination with a desorption light source of  $h\nu_{x2} = 2.71$  eV. As shown in Fig. 4a, the PL intensity in the region  $h\nu_{em} < h\nu_{x2}$  (curve X') decreased relative to that observed in the absence of desorption light (curve X). The difference in PL intensity,  $I_{diff}$ , between X and X' (Fig. 4b) clearly shows the decrease in the PL intensity of X' at energies less than  $h\nu_{x2}$ , indicating near-field desorption as described in Fig. 1a.

Using a desorption light source with  $h\nu_{x2} = 2.33$  eV, which is lower in energy than the peak PL of deposited InGaN (2.5 eV) in the absence of desorption light, similar decreases in PL intensity were observed for  $r_{TEI} = 2.5 \times 10^{-3}$  sccm and  $r_{TEI} = 5.0 \times 10^{-3}$  sccm (curves Y' and Z' in Fig. 5a, respectively). The difference in PL between Y and Y', and Z and Z', as indicated by curves Y'' and Z'' in Fig. 5b, respectively, shows that the PL intensity of both Y'

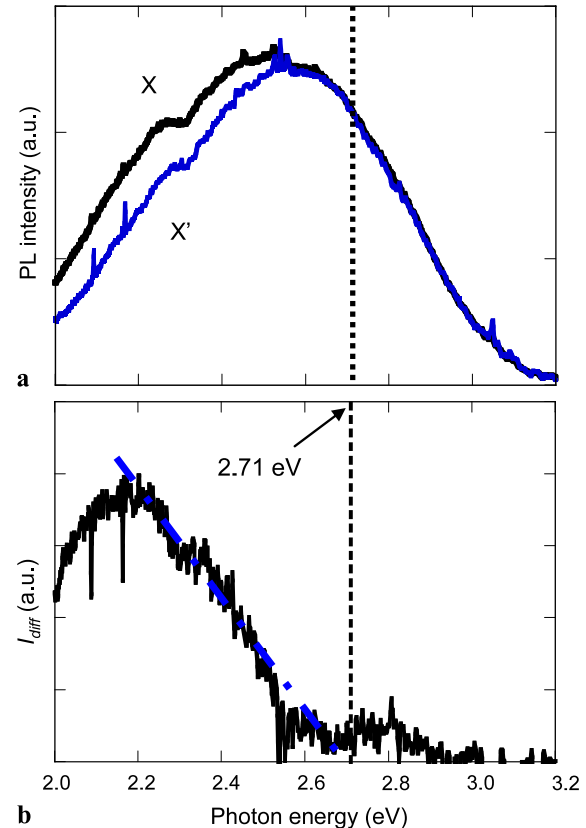


**Fig. 4** Spectral changes induced by desorption light illumination at 2.71 eV during PECVD. **a** PL spectra were obtained at 5 K using room-temperature PECVD with  $r_{TEI} = 2.5 \times 10^{-3}$  (curves X and X') and a desorption source energy of  $h\nu_{x2} = 2.71$  eV. **b** The difference spectrum shown for X–X'

and Z' decreased at energies below  $h\nu_{x2} = 2.33$  eV. In addition, Fig. 5b shows that higher levels of  $r_{TEI}$  (curve Z'') resulted in increased  $I_{diff}$  values at  $h\nu_{x2} > 2.33$  eV relative to those obtained at lower  $r_{TEI}$  (curve Y''). This further indicates In desorption. This result confirms that the use of the desorption light source during film deposition did not permit additional In doping other than that determined by the pho-

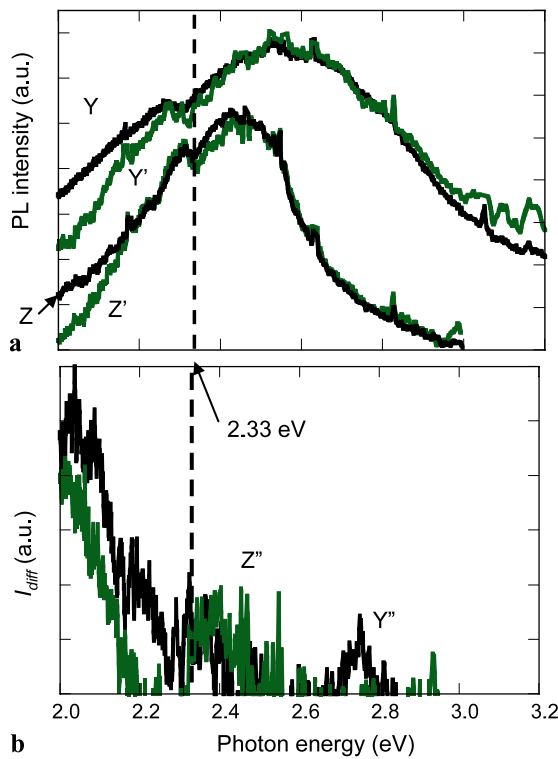


**Fig. 5** Spectral changes induced by desorption light illumination at 2.33 eV during PECVD. **a** PL spectra were obtained at 5 K using room-temperature PECVD with  $r_{TEI} = 2.5 \times 10^{-3}$  (curves Y and Y') and  $5.0 \times 10^{-3}$  (curves Z and Z') sccm and a desorption source energy of  $h\nu_{x2} = 2.33$  eV. **b** The PL difference spectra shown for Y-Y' (curve Y'') and Z-Z' (curve Z'')

ton energy of the desorption light source itself. This effect resulted in a film with a more spatially uniform In content.

## 5 Conclusion

Since the deposition method described herein is based on a photo-desorption reaction, it can be applied with other deposition techniques, such as MOCVD [1], molecular beam epitaxy [11] and pulsed-laser depositions [12], and can also be applied with other compound semiconductors such as In-GaAs [13].

## References

1. S. Nakamura, *Science* **281**, 956 (1998)
2. K.J. Vahala, *Nature* **424**, 839 (2003)
3. S. Nizamoglu, T. Ozel, E. Sari, H.V. Demir, *Nanotechnology* **18**, 065709 (2007)
4. T. Kawazoe, K. Kobayashi, S. Takubo, M. Ohtsu, *J. Chem. Phys.* **122**, 024715 (2005)
5. T. Yatsui, W. Nomura, M. Ohtsu, *Nano Lett.* **5**, 2548 (2005)
6. S. Yamazaki, T. Yatsui, M. Ohtsu, *Appl. Phys. Exp.* **1**, 061102 (2008)
7. H. Okabe, M.K. Emadi-Babaki, V.R. McCrary, *J. Appl. Phys.* **69**, 1730 (1991)
8. K. Watanabe, *J. Chem. Phys.* **22**, 1564 (1954)
9. M.D. McCluskey, C.G. Van de Walle, C.P. Master, L.T. Romano, N.M. Johnson, *Appl. Phys. Lett.* **72**, 2725 (1998)
10. A. Koukitu, H. Seki, *Jpn. J. Appl. Phys.* **35**, L1638 (1996)
11. R. Singh, D. Doppalapudi, T.D. Moustakas, L.T. Romano, *Appl. Phys. Lett.* **70**, 1089 (1997)
12. A. Kobayashi, J. Ohta, H. Fujioka, *J. Appl. Phys.* **99**, 123513 (2006)
13. K. Akahane, N. Ohtani, Y. Okada, M. Kawabe, *J. Cryst. Growth* **245**, 31 (2002)